Optics and Lasers in Engineering 62 (2014) 132–138

Contents lists available at ScienceDirect

Optics and Lasers in Engineering

journal homepage: www.elsevier.com/locate/optlaseng

# Laser polarization-assisted diffusion for modifying electromagnetic properties of metals

Sen-Yong Chen [a], Othmane Benafan [b,1], Raj Vaidyanathan [b], Aravinda Kar [a,*]

[a] Laser-Advanced Materials Processing Laboratory; Center for Research and Education in Optics and Lasers (CREOL), The College of Optics and Photonics, University of Central Florida, Orlando, FL 32816, USA

[b] Advanced Materials Processing and Analysis Center (AMPAC); Mechanical, Materials, and Aerospace Engineering, University of Central Florida, Orlando, FL 32816, USA

ARTICLE INFO

*Article history:*
Received 26 December 2013
Received in revised form
25 March 2014
Accepted 28 May 2014
Available online 21 June 2014

*Keywords:*
Electromagnetic property
Laser polarization
Magnetic field
Platinum diffusion
Beam shaping

ABSTARCT

Laser diffusion has previously been studied to incorporate dopants in semiconductors and to carburize steel for surface hardening without melting the substrate, among others. The optical and electromagnetic properties of materials can also be modified by this diffusion method to tailor the material response at different frequencies of the electromagnetic spectrum. Platinum atoms have been diffused into titanium and tantalum sheets by a laser chemical vapor diffusion method using a metallorganic compound of platinum and laser beams of different polarizations. Thermal decomposition of the precursor at the laser-heated spot on the surface of the substrate generates platinum atoms that diffuse into the substrate, producing laser-platinized samples. The transmittances of the samples are determined by measuring the strength of the transmitted magnetic field oscillating at 63.86 MHz. The laser-platinized samples produced by linearly polarized lasers exhibit higher transmittances than the samples obtained by using azimuthally polarized lasers.

Published by Elsevier Ltd.

## 1. Introduction

The optical and electromagnetic properties of materials at different frequencies of the electromagnetic spectrum have been widely used in many applications such as communications, imaging and remote sensing. Laser chemical vapor diffusion has been used to dope semiconductors for fabricating semiconductor devices such as light-emitting diodes, [1] gas sensors [2] and transistors, [3] and to modify the surface chemistry for improved mechanical properties such as hardness. In this diffusion process, the substrate is generally heated with a laser beam in a vacuum chamber containing the vapor of a suitable metallorganic precursor of the dopant atoms, resulting in thermal decomposition of the precursor, production of the dopant atoms and subsequent diffusion of the atoms into the substrate. The advantage of this process is that the rapid heating and cooling inherent in laser processing provides a nonequilibrium diffusion mechanism to achieve higher dopant concentration in the substrate than the solid solubility limit of the substrate [1]. Similar to altering the properties of semiconductors, the electromagnetic properties of metals can also be modified by the laser chemical vapor diffusion method to tailor the material response, such as reflection and transmission, at different frequencies of the electromagnetic spectrum [4]. Laser heating can be used to incorporate diffusant atoms into the substrate. It can also be used to induce solid state diffusion among the constituent atoms of the substrate to form new crystalline phases for enhancing material properties.

To produce a diffused layer of impurities in metals, the conventional solid state diffusion process, which occurs under isothermal conditions in a furnace, is not applicable in many cases where the mechanical properties such as the yield and fatigue strengths are affected due to prolonged exposure to high temperatures. The laser diffusion technique is a non-isothermal solid state diffusion process without melting the substrate. Diffusion can be accomplished at much higher localized temperatures at shorter durations than in the conventional furnace-based diffusion process. This non-isothermal, localized high-temperature diffusion mechanism increases the diffusion coefficient and concentration of impurities with minimal changes in the mechanical properties of the substrate. The laser irradiance, laser-substrate interaction time and reflectivity of the substrate are generally studied for modifying the properties of materials by laser heating. Polarization is another important property of lasers that can be useful for changing the structures of materials.

Laser polarization represents the direction traced by the tip of the oscillating electric field of the laser over one period of oscillation on a plane perpendicular to the direction of propagation of the laser.

* Corresponding author.
*E-mail address:* akar@creol.ucf.edu (A. Kar).
[1] Presently at NASA Glenn Research Center, Structures and Materials Division, Cleveland, OH 44135.

http://dx.doi.org/10.1016/j.optlaseng.2014.05.012
0143-8166/Published by Elsevier Ltd.

Petring et al. [5] showed that the absorptivity of the workpiece depends on polarization in laser cutting. Niziev and Nesterov [6] studied the efficiency of cutting as a function of laser polarization and achieved higher efficiency with a radially polarized laser than with a linearly or circularly polarized laser for cutting metal sheets with large aspect ratios. Ho [7] calculated the absorbed laser energy for keyhole welding and drilling applications where the laser undergoes single reflection in a certain region of the cavity or multiple reflections in other regions. The absorbed energy per unit area is the highest for *s*-polarization in the single reflection zone, whereas the total absorbed energy is the highest for *p*-polarization in the multiple reflection zone. The polarization allows to modify the properties of material by two mechanisms: (i) a thermal effect in which the polarization-dependent absorption of laser energy affects the temperature distribution in the substrate and, consequently, the impurities are thermally activated for the diffusion process, and (ii) a phonon effect in which the electric field of the laser can restrict the vibrational motions of the impurities to certain directions and, therefore, the diffusant atoms migrate in an organized manner instead of moving randomly. Artsimovich et al. [8] obtained higher diffusion coefficient of oxygen in Si with a laser beam of polarization parallel to the Si–O–Si bonds. Pavlovich [9] presented a theory to explain the enhanced diffusion coefficient of oxygen in Si and concluded that the enhancement occurs when the quantum of energy and the vibrational energy of Si lattice are comparable and the direction of polarization is parallel to the direction of antisymmetric vibration of oxygen atoms along $<111>$.

## 2. Experimental studies

### 2.1. Laser platinum diffusion

To incorporate Pt into a metal substrate, a metallorganic precursor, platinum(II) acetylacetonate [$Pt(C_5H_7O_2)_2$ or $Pt(acac)_2$], is selected as the precursor because it is less toxic and its thermal decomposition temperature is relatively low 210–240 °C [10]. The products of the thermochemical reaction [11,12] are Pt atoms and acetylacetone ($CH_3COCH_2COCH_3$). Pt is diffused into Ti and Ta substrates using the laser chemical vapor diffusion process. Ti and Ta are biocompatible materials with applications in medical treatments such as orthopedic and orthodontic applications. Often Ti plates and pins are used to repair fractured bones. Pt is also a biocompatible material. Tailoring the electromagnetic properties (e.g., transmittance) of Ti and Ta using Pt would enable nondestructive testing of these materials for detecting surface or internal defects when medical parts are produced using Ti or Ta. The electromagnetic response of these materials would also be useful for noninvasive medical examination of patients wearing implants made of these materials.

Each substrate was a 20 mm square sheet of thickness 25 or 50 μm. To avoid any bending or distortion of the sheets during laser heating, four edges of the substrate were clamped between two aluminum plates. Each plate had a square hole of side 18 mm. These two aluminum plates were placed on top of another aluminum plate without a hole. Therefore, only one side of the Ti and Ta sheets was accessible for laser heating and incorporation of Pt atoms. The clamped substrate was placed in a vacuum chamber as shown in Fig. 1 to carry out laser diffusion experiments. 200 mg of the Pt precursor was dissolved in 20 ml of acetylacetone and a bubbler was used to heat the solution with a hot plate by maintaining the temperature of the hot plate at 130 °C. The pressure of the vacuum chamber was lowered to about $10^{-3}$ Torr and the vapor of the precursor solution was then delivered to the chamber with argon gas until a total pressure of 2 atm was achieved inside the chamber. A Nd:YAG laser of wavelength 1064 nm was used for heating the substrate to cause thermal decomposition of the Pt precursor at the laser–substrate interaction zone and for diffusion of Pt atoms into the substrate.

The temperature of the substrate can be varied by changing various processing parameters such as the laser irradiance and scanning speed. The Ti substrates were irradiated with a laser beam of power $P_L=12$ W for two scanning speeds $u=6$ and 12 mm/s and two polarizations at each speed. The Ta substrates, however, required more energy to be sufficiently hot for the formation and diffusion of Pt into the substrate than in the case of the Ti sheets due to different thermophysical properties of these two metals. Therefore the Ta substrates were irradiated with a laser beam of power $P_L=16$ W for two scanning speeds $u=3$ and 6 mm/s and two polarizations at each speed. Thick samples require more energy than thin samples for the same increase in temperature and the reflectivity of rough surfaces is less than that

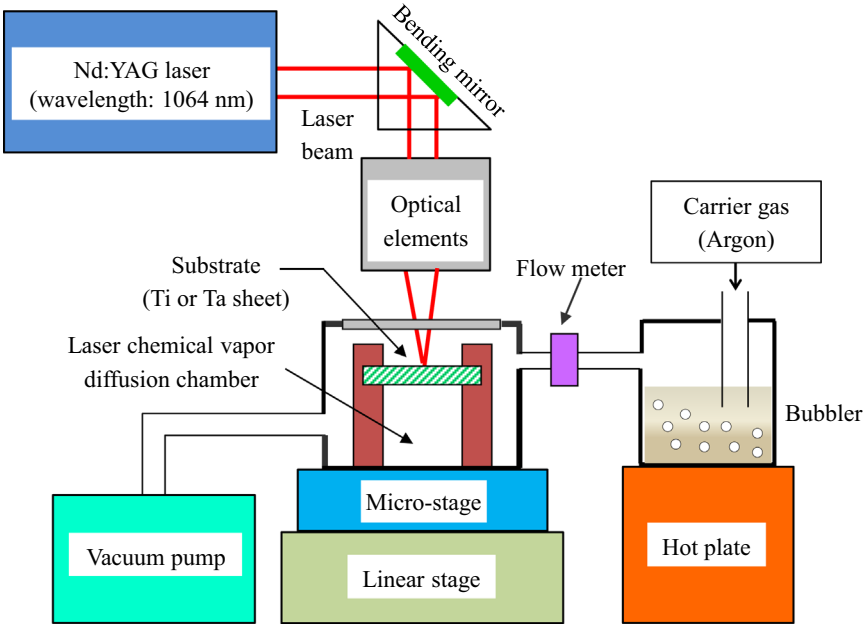


**Fig. 1.** Schematic of a laser chemical vapor diffusion system to incorporate diffusant atoms into substrates.

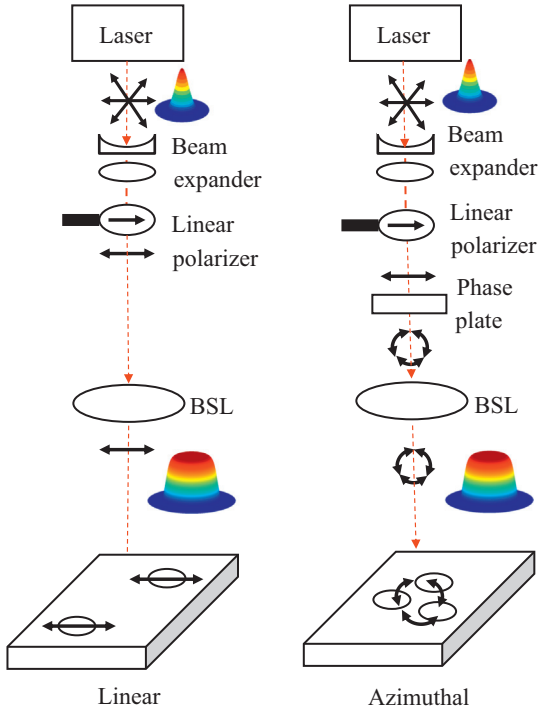


**Fig. 2.** Optical elements used to generate polarized flat-top laser beams: (a) linear polarization and (b) azimuthal polarization.

of smooth surfaces. Therefore the Ta substrates of 50 μm thickness were roughened with sandpaper (Grade 2000) to increase the absorption of the laser energy. The laser beam diameter was 2 mm on the substrate surface for all the diffusion experiments. For each thickness (25 μm or 50 μm) and each scanning speed, two sheets of Ti and Ta were laser-treated to incorporate Pt into the sheets and the composition of various elements were determined by Electron Dispersive Spectroscopy (EDS) at ten randomly selected spots on each sheet.

To understand the effect of laser polarization on the diffusion of Pt and, consequently, on the electromagnetic properties of Ti and Ta, linear and azimuthal polarizations of the Nd:YAG laser beam were tested. These two polarizations were produced from the original unpolarized Nd:YAG laser using optical elements, and a beam shaping lens was used to transform the incident Gaussian irradiance profile into a flat-top laser beam as shown in Fig. 2. A linearly polarized flat-top laser beam was generated using a linear polarizer and a beam shaping lens. An azimuthally polarized flat-top beam was formed using a linear polarizer, a phase plate [13] and a beam shaping lens.

### 2.2. Reflectivity measurements for Ti and Ta sheets at the Nd:YAG laser wavelength of 1064 nm

To estimate the temperature of the laser–substrate interaction zone where thermal decomposition of the Pt precursor occurs, the reflectivities of the Ti and Ta substrates are important because they significantly influence the amount of laser energy utilized for heating the substrates. Although the laser beam was normal to the substrates during the laser Pt diffusion experiments, the reflectivity measurements were carried out at an angle of incidence of the laser beam of approximately 5° for convenience in measuring the laser power. The Ti and Ta samples were tilted slightly to allow separation between the incident and reflected laser beams and the powers of these two beams were measured using a power meter. The diameter of the active region of the detector was 2.54 cm and the detector was moved to scan three-dimensionally to capture

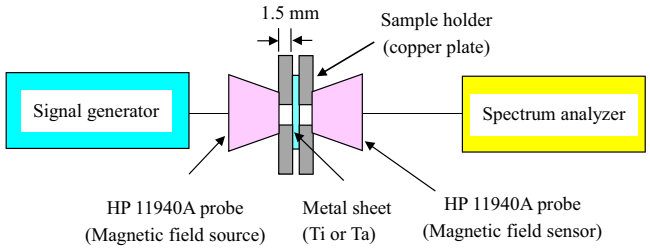


**Fig. 3.** Apparatus for measuring magnetic field strength to determine the transmittance and reflectance of Ti and Ta sheets.

any diffusely reflected laser energy. The large diameter of the detector enabled capturing the entire reflected beam in the direction of specular reflection. The ratio of the reflected power to the incident power yields the reflectivity of the sample.

### 2.3. Transmission measurements at 63.86 MHz frequency of the magnetic field

Transmittance is an important property for nondestructive evaluation of internal defects in solid materials and for nonintrusive medical care of patients treated with metallic implants. Since 63.86 MHz frequency is widely used in magnetic resonance imaging systems, the electromagnetic response of various biocompatible materials at this frequency is of interest. To measure the transmission of magnetic fields oscillating at a frequency of 63.86 MHz, each laser-platinized sample was held between two copper plates having a square window of side 15 mm at the center of each plate. The length, width and thickness of each of the copper plates were 100, 70 and 1.5 mm, respectively, to block the permeation of the magnetic field lines from a source to a sensor of the magnetic field. The platinized sample was placed between two HP 11940A probes as shown in Fig. 3 and one of the probes was a source of the magnetic field while the other was a sensor of the field. This setup enables the magnetic field generated by the source to propagate through the front window, pass through the sample and exit through the rear window so that the transmitted magnetic field can be detected by the sensor. A signal generator, which produces alternating current signals at a frequency of 63.86 MHz, was connected to the source probe to create a magnetic field at this frequency. The amplitude of the transmitted magnetic field was measured with a spectrum analyzer by connecting it to the sensor probe. Since the transmittance is the ratio of the transmitted to incident magnetic fields, the amplitude of the incident magnetic field was measured in the absence of any sample in the window.

### 2.4. Electrical conductivity measurements

The transmittance of a material can change after laser treatment due to several reasons. If other elements such as carbon and oxygen are present in the sample, they can produce dielectric microstructures in the form of carbides and oxides during the laser treatment at high temperatures. These dielectric materials may absorb less of the magnetic field and thereby enhance the transmittance of the sample. On the other hand, Pt can increase the electrical conductivity of Ti and Ta samples since the electrical conductivity of Pt is higher than those of Ti and Ta. Therefore Pt can increase the reflectivity of the sample, resulting in less magnetic energy available for transmittance through the sample.

The direct current (DC) electrical conductivity of each sample was measured [14] using a four-probe method as shown in Fig. 4. When a constant current $I$ is supplied through the two outer current probes $C_1$ and $C_2$, and the voltage $V$ is measured across the

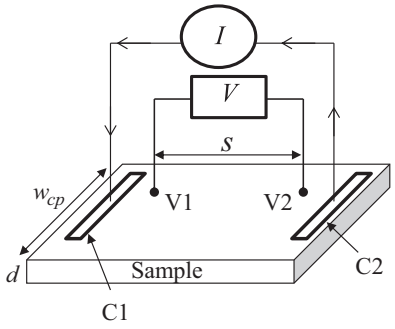


**Fig. 4.** Illustration of four-point method used to measure the conductivity of metal sheets.

two inner voltage probes $V_1$ and $V_2$, the DC electrical conductivity $\sigma_{DC}$ of the sample can be determined by the following expression:

$$\sigma_{DC} = K\frac{I}{V}\frac{s}{w_{cp}d} \tag{1}$$

where $K$ is a correction factor that depends on the geometries of the samples and current probes, $s$ is the separation between the two voltage probes $V_1$ and $V_2$, $w_{cp}$ is the width of the current probe and $d$ is the thickness of the sample. In this study, $s=15$ mm, $w_{cp}=20$ mm, and $d=25$ or 50 μm depending on the laser-platinized samples used for a particular measurement. The value of $K$ was estimated by calibrating the four-probe instrument using a thin copper sheet of known DC electrical conductivity [15], $5.7\times10^7\ \Omega^{-1}\,m^{-1}$, and by measuring $I$ and $V$ for the copper sheets of the same dimensions as the Ti and Ta samples used in this study. Substituting these data into Eq. (1), the values of $K$ were found to be 1.043 and 1.029 for 25 and 50 μm thick sheets, respectively.

## 3. Results and discussion

The reflectivities of the Ti and Ta samples were measured for two polarizations in order to estimate the surface temperatures and select appropriate laser parameters for carrying out laser diffusion experiments without melting the substrates. Fig. 5 shows the reflectivity data for azimuthal (Az) and linear ($L_\perp$) polarizations with the linear polarization being perpendicular to the laser scanning direction. The surface roughnesses of the samples are also presented in Fig. 5, showing that the reflectivity decreases as the surface roughness increases. In the case of 50 μm Ta sheets, the reflectivity of the roughened sheet is lower than that of the as-received sheet since the surface roughness increases due to mechanical roughening with a sandpaper. The experimental data are compared with the Fresnel reflectivity at normal incidence, which is given by $R_F=|\tilde{n}-1/\tilde{n}+1|^2$, where $\tilde{n}$ is the complex refractive index of the Ti or Ta sheets. This expression is applicable to homogeneous and isotropic materials with a smooth surface. Since the surface roughnesses of the Ti samples are small with respect to the incident laser wavelength, the reflectivities of Ti samples are close to the corresponding Fresnel reflectivity. The reflectivities of Ta samples, however, are about one-half of the corresponding Fresnel reflectivity since their roughnesses are large with respect to the laser wavelength.

These reflectivity data are used in the following equation to estimate the substrate surface temperature during the laser diffusion experiment:

$$T_s = T_i + \frac{P_L(1-R)\tau}{2r_0u\tau d\rho C_p + 2r_0u\tau^2h + 2u\tau^2dh_l} \tag{2}$$

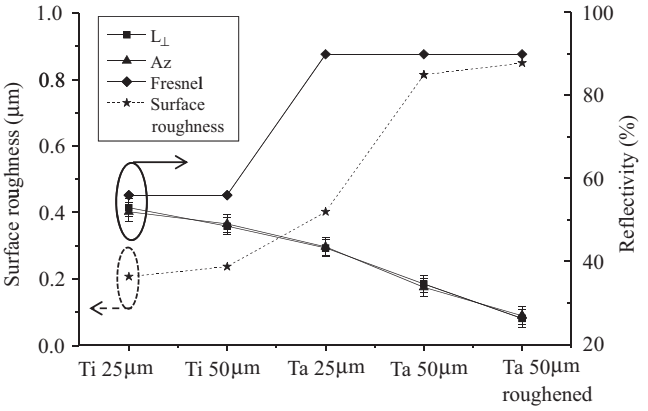


**Fig. 5.** Surface roughness of Ti and Ta samples and corresponding reflectivity at the wavelength of 1064 nm for two polarizations.

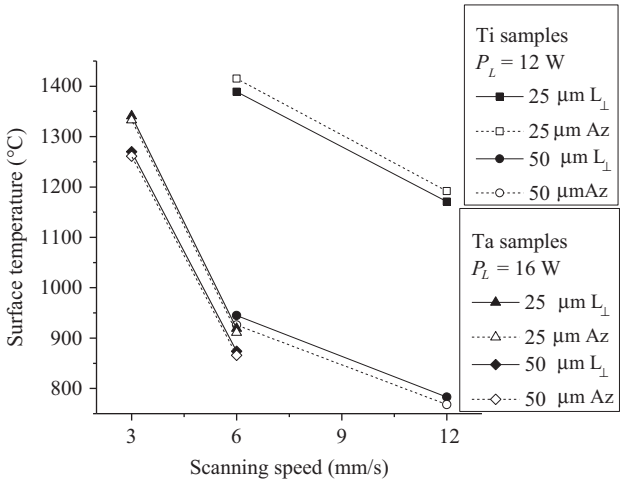


**Fig. 6.** Predicted surface temperature of Ti and Ta sheets.

where $T_s$ and $T_i$ are the surface and initial temperatures of the substrate of thickness $d$, respectively, which is irradiated with a laser beam of power $P_L$, $R$ and $\tau$ are the reflectivity and laser-substrate interaction time ($2r_0/u$), respectively, $r_0$ is the laser beam radius and $u$ is the laser scanning speed, $\rho$ and $C_p$ are the density and specific heat capacity of the samples, respectively, $h$ is the heat transfer coefficient at the surface of the substrate and $h_l$ is the lateral heat transfer coefficient of the substrate. Typical heat transfer coefficients range from 5 to 30 $W/m^2\,K$ in atmospheric air [16]. However, $h$ was chosen as 200 $W/m^2\,K$ because the gas pressure inside the chamber was 2 atm. $h_l$ was taken to be $k_{th}/r_0$, where $k_{th}$ is the thermal conductivity of the sample, since the heat loss in the lateral direction occurs due to conduction through the workpiece. The densities, thermal conductivities and specific heat capacities of Ti and Ta are 4500 and 16600 $kg/m^3$, 21.9 and 57.5 W/m K, and 522 and 140 J/kg K, respectively [17], and $h_l=2.2\times10^4$ and $5.8\times10^4\ W/m^2\,K$ for Ti and Ta, respectively. Based on these data, the calculated surface temperatures are plotted in Fig. 6 showing that the surface temperature is higher for three cases: (i) lower scanning speed, (ii) lower reflectivity and (iii) thinner sample.

The laser-platinized samples were tested for the transmission of a magnetic field oscillating at 63.86 MHz using magnetic field apparatus shown in Fig. 3. The magnetic field sensor produces a voltage signal due to the transmitted time-varying magnetic field and this response ($H'$) was measured in units of dB μV. A scaling factor of the spectrum analyzer, $10^{(H'+48.5)/20}$, was applied to $H'$ to determine the magnetic field strength in units of μA/m for the

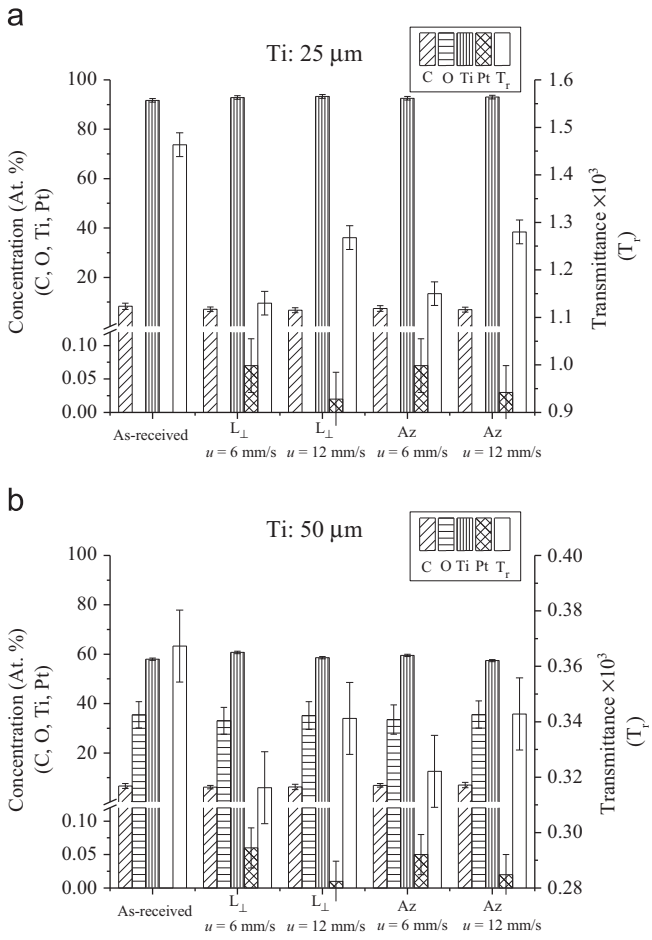


**Fig. 7.** Transmittance and impurity concentration of Ti samples for two different thicknesses: (a) 25 μm and (b) 50 μm. The error bars are based on two samples with ten randomly selected spots on each of them for measuring the composition of various elements.

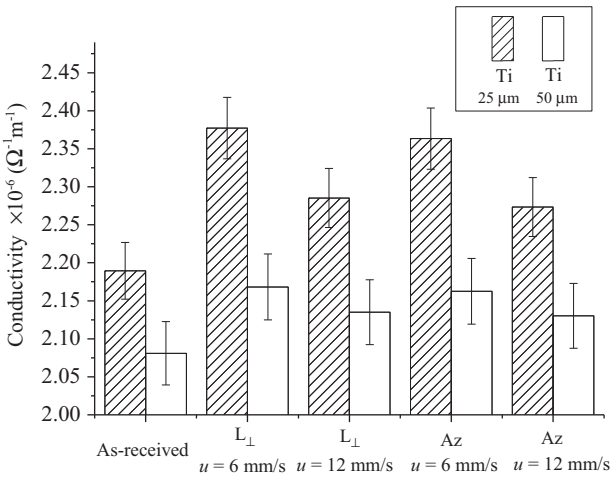


**Fig. 8.** Measured DC electrical conductivity of Ti sheets.

incident magnetic field $\tilde{H}_{in}$ and the transmitted magnetic field $\tilde{H}_t$. These data were used to determine the experimental transmittance $(\tilde{T})$ of different samples using the expression $\tilde{T} = \tilde{H}_t/\tilde{H}_{in} \times 100\%$.

The transmittance data of Ti samples are presented in Fig. 7 with the corresponding Pt concentrations in the samples to examine the effect of polarizations. EDS was used to determine the Pt concentrations in the samples. Although the error bars are fairly large, Pt peaks were observed in the EDS data indicating the presence of Pt in the samples. The error bars were obtained by examining ten randomly selected spots on a large laser-treated area. Pt was not observed in certain spots, indicating that either the amount of Pt was below the detection limit of the EDS system or Pt was absent at that spot. Therefore the error bars are indicative of nonuniform distribution of Pt at the sample surface in this study. The diffused Pt atoms modify the interaction between the magnetic field and the Ti sample, which is evident in Fig. 7 showing lower transmittances of platinized Ti than the as-received sample. However, any variation in the compositions of carbon and oxygen can also affect the transmittance. Fig. 7a and b shows that the compositions of carbon and oxygen atoms decrease in the laser-treated Ti sheets of thicknesses 25 μm and 50 μm, respectively, compared to the corresponding as-received samples. Generally carbon and oxygen atoms form carbides and oxides which are dielectrics enabling the transmission of magnetic fields with little absorption. Therefore, the reduction in the transmittance of the laser-treated Ti sheets may be due to diffused Pt that increases the electrical conductivity of the sample and, consequently enhancing its reflectivity. Increased DC electrical conductivity of the platinized samples is shown in Fig. 8. Incorporation of Pt into Ti increases the electrical conductivity of Ti since the conductivity of Pt ($9.26 \times 10^6\ \Omega^{-1}\ m^{-1}$) is higher than that of Ti ($2.38 \times 10^6\ \Omega^{-1}\ m^{-1}$) [17]. Higher Pt concentration in the Ti samples, which occurs due to higher surface temperatures at lower scanning speeds, causes higher conductivity and lower transmittance. Since the surface temperature of thinner samples is higher than that of thicker samples, higher Pt concentration is observed in the 25 μm thick Ti samples than in the 50 μm thick Ti samples.

The transmittance of Ti is lower for linearly polarized laser-treated samples than for the case of azimuthal polarization, which may be due to different mechanisms in the interaction between the electric field of the laser and the phonons of the material. Since the electric field can polarize atoms, the oscillating electric field of a laser beam can influence the oscillations of Pt and Ti atoms in the samples. In the case of linearly polarized laser beams, the electric field, which oscillates in the same direction during the laser diffusion process, can excite the local vibration modes of Pt and Ti atoms, resulting in more diffusion of Pt and, consequently, higher conductivity and lower transmittance of the sample. Additionally the linearly polarized laser beam with polarization perpendicular, i.e., transverse, to the laser scanning speed, provides a mechanism to oscillate the Pt atoms in this transverse direction. Consequently, the Pt atoms can disperse in the transverse direction as the laser beam moves. This dispersion may cause less collisional energy loss and enable the Pt atoms to utilize most of their vibrational energy for migration with higher jump frequency in the transverse direction and into the substrates. In the case of azimuthal polarization, however, the oscillation direction of the electric field is tangential to the circumference of the circular beam, i.e., the electric filed oscillates in the angular direction in polar coordinates, which polarizes the motion of Pt and Ti atoms to the tangential direction in polar coordinates. Due to this circumferential oscillation of the atoms and since the laser beam moves relative to the substrate, the movements of the atoms may be partially random, i.e., neither completely organized nor completely random. So the local vibration modes of Pt and Ti atoms are not excited significantly to enhance the migration of Pt atoms in the substrates. An opposite trend, however, is observed in the case of the laser scanning speed $u = 12$ mm/s where the concentration of Pt in Ti is lower for linear polarization than for azimuthal polarization. This trend may be attributed to very low concentration of Pt for which the effect of laser polarization on Pt diffusion is negligible.

For Ta sheets, the transmittance and impurity concentration are plotted in Fig. 9 and the DC electrical conductivity is presented in

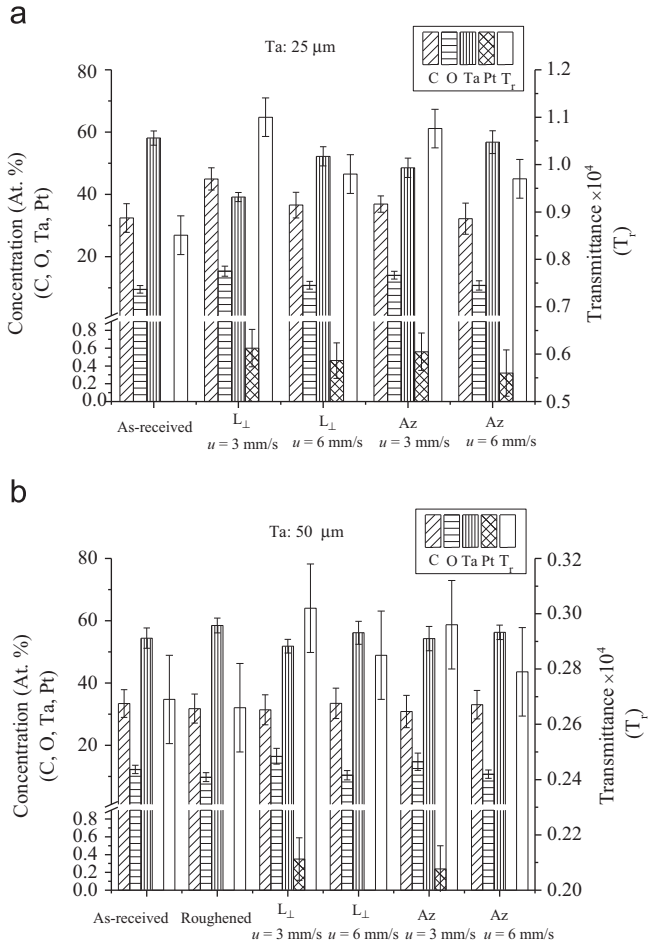


**Fig. 9.** Transmittance and impurity concentration of Ta samples for two different thicknesses: (a) 25 μm and (b) 50 μm. The error bars are based on two samples with ten randomly selected spots on each of them for measuring the composition of various elements.

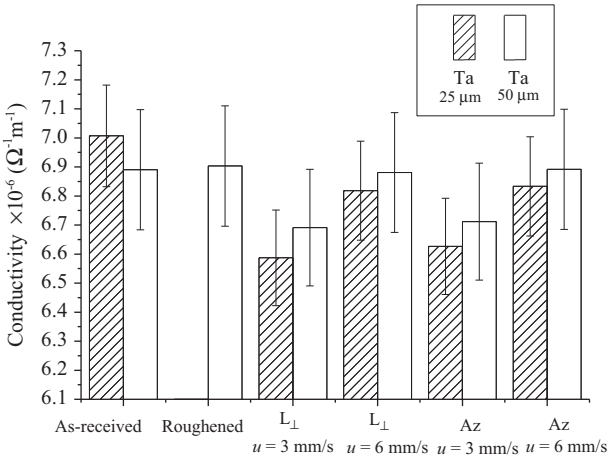


**Fig. 10.** Measured DC conductivity of Ta sheets.

Fig. 10 for two polarizations. The transmittances are higher for platinized Ta samples than for the as-received sample. Also the DC electrical conductivities are lower for platinized Ta samples than for the as-received sample. These results are opposite to the trend observed for Ti samples. Fig. 9, however, shows that Pt atoms are present in the laser-treated Ta samples, which should increase their electrical conductivity. The effect of Pt atoms for increasing the conductivity of Ta may not be as much as in the case of Ti because the electrical conductivity of Pt ($9.26\times10^6\,\Omega^{-1}\,m^{-1}$) is very close to Ta ($7.41\times10^6\,\Omega^{-1}\,m^{-1}$) than to Ti ($2.38\times10^6\,\Omega^{-1}\,m^{-1}$) [17]. The increased concentration of oxygen in the laser-treated Ta samples, therefore, dominates the modification of the properties of Ta, resulting in lower electrical conductivity and higher transmittance. Oxygen may be present in the form of tantalum oxide which is a dielectric material allowing much of the magnetic field to transmit through the sample. For Ta samples that are laser-treated at the lower scanning speed, the transmittance is found to increase because the temperature of the substrate increases as the scanning speed decreases, and the oxidation increases with temperature.

Similarly the concentration of Pt in Ta samples is higher at the lower scanning speed due to higher surface temperature. The surface temperature of the 25 μm thick Ta samples is higher than that of the 50 μm thick Ta samples and, therefore, the concentration of Pt is higher in the former samples than in the latter samples. Also the concentration of Pt is slightly higher in the linearly polarized laser-treated Ta samples than in the case of the azimuthally polarized laser treatment. This effect of polarization may be attributed to aligning the atomic vibrations to certain directions and exciting the local vibration modes of Pt and Ta atoms.

It should be noted that Fig. 9b does not show any Pt concentration for the roughened sample because an as-received Ta sample was roughened and its composition and transmittance were determined before laser-treating the sample. The roughened samples were subsequently laser-treated for Pt diffusion experiments. Thus the initial roughened sample provides reference data for the laser-treated samples. Also Fig. 9b does not show Pt concentrations for 50 μm thick Ta samples, which were treated with linearly and azimuthally polarized laser beams at the scanning speed of 6 mm/s, because the concentrations were below the detection limit of the EDS system. However Pt can be observed in the 25 μm thick Ta samples laser-treated at the scanning speed of 6 mm/s as shown in Fig. 9a. It can also be observed in Fig. 9a and b that the average amount of Pt is less in the 50 μm thick Ta sample than in the 25 μm thick Ta sample for the scanning speed of 3 mm/s. This trend may be attributed to surface effects, particularly the chemical reaction and diffusion, occurring at the rough surface of the 50 μm thick Ta sample compared to the smooth surface of the 25 μm thick Ta sample.

For efficient production of Pt atoms at the sample surface and its subsequent diffusion into the sample, the reactant (i.e., the metallorganic Pt precursor) molecules need to diffuse to the laser-substrate interaction zone and the reaction products except Pt need to diffuse out of the interaction zone enabling fresh reactant to enter into the interaction zone. This diffusive transport of the reactant and reaction products generally involves surface diffusion, i.e., diffusion at the sample surface, and bulk diffusion, i.e., diffusion from the precursor vapor phase. The asperities of a rough surface can impede surface diffusion compared to a smooth surface. Additionally, the troughs of a rough surface may reduce the accessible surface area for chemical reaction compared to a smooth surface since the reaction products generated at the crests can diffuse into the troughs preventing fresh reactants from reaching the troughs by bulk diffusion. Also the reaction products may not diffuse out of the troughs of a rough surface as readily as from a smooth surface. These factors contribute to lowering the Pt composition as observed for the rough sample in Fig. 9b.

## 4. Conclusion

Platinum has been diffused into Ti and Ta sheets using a Nd:YAG laser. The polarization of the laser is modified to produce linearly or azimuthally polarized beams to carry out laser chemical vapor diffusion experiments. The effect of impurities on the

transmission of a magnetic field oscillating at the frequency 63.86 MHz is examined. Pt decreases the transmittance of Ti and oxygen increases the transmittance of Ta compared to the respective as-received samples.

For laser-treated Ti samples, the reduction in the transmittance may be attributed to increased DC electrical conductivity due to two effects. Since the electrical conductivity of Pt is significantly higher than that of Ti, the diffused Pt atoms reduce the transmittance of the Ti sheets by increasing the electrical conductivity of the sheets. The second effect arises from the laser polarization. Linearly polarized lasers can restrict the lattice oscillation to certain directions and excite the local vibration modes of Pt and Ti atoms to increase the diffusion of Pt into the Ti sheets with the consequence of higher conductivity and lower transmittance of the samples.

For laser-treated Ta samples, the diffused Pt atoms do not increase the electrical conductivity of Ta as much as in the case of Ti because the conductivities of Pt and Ta are almost the same. However the transmittance of the treated samples increases compared to the as-received sample, which may be attributed to increased oxygen concentration in the samples. The presence of oxygen can form $TaO_2$, inducing dielectric properties in the samples. This transformation raises the transmittance of the Ta samples since the magnetic field can propagate through the samples without being absorbed.

## References

[1] Bet S, Quick NR, Kar A. Laser doping of chromium in 6H-SiC for white light-emitting diodes. J Laser Appl 2008;20:43–9.
[2] Lim G, DeSilva UP, Quick NR, Kar A. Laser optical gas sensor by photoexcitation effect on refractive index. Appl Opt 2010;49:1563–73.
[3] Weiner KH, Sigmon TW. Thin-base bipolar transistor fabrication using gas immersion laser doping. IEEE Electron Device Lett 1989;10:260–3.
[4] S-Y Chen, O Benafan, R Vaidyanathan and A Kar, Electromagnetic properties of metals based on transmission measurements at 64 MHz. In: Kassab AJ AD, editors. Proceedings of ICIPE, CENTECORP Publishing, Orlando; (2011). p. 61–5.
[5] D Petring, P Abels and E Beyer, Absorption distribution on idealized cutting front geometries and its significance for laser beam cutting. In: Quenzer A, editor. Proceedings of SPIE, High Power $CO_2$ Laser Systems and Applications, 1020, SPIE, Bellingham; (1988). p. 123–31.
[6] Niziev VG, Nesterov AV. Influence of beam polarization on laser cutting efficiency. J Phys D: App. Phys 1999;32:1455–61.
[7] Ho C-Y. Effects of polarizations of a laser on absorption in a paraboloid of revolution-shaped welding or drilling cavity. J Appl Phys 2004;96:5393–401.
[8] MV Artsimovich, AN Baranov, VV Krivov, Eugene M Kudriavtsev, Emma N Lotkova, BH Makeev, et al., Resonant IR laser-induced diffusion of oxygen in silicon. In: Proceedings of SPIE 1397 Eighth International Symposium on Gas Flow and Chemical Lasers, SPIE, Madrid; (1991). p. 729–33.
[9] Pavlovich VN. Influence of radiation polarization on laser-enhanced resonance diffusion in crystals. Sov Phys Solid State 1990;32:1315–7.
[10] Morozova NB, Zharkova GI, Semyannikov PP, Sysoev SV, Igumenov IK, Fedotova NE, et al. Vapor pressure of precursors for CVD on the base of platinum group metals. J Phys IV Fr 2001;11:609–16.
[11] Thurier C, Doppelt P. Platinum OMCVD processes and precursor chemistry. Coord Chem Rev 2008;252:155–69.
[12] Hoene JV, Charles RG, Hickam WM. Thermal decomposition of metal acetylacetonates: mass spectrometer studies. J Phys Chem 1958;62:1098–101.
[13] Machavariani G, Lumer Y, Moshe I, Meir A, Jackel S. Efficient extracavity generation of radially and azimuthally polarized beams. Opt Lett 2007;32:1468–70.
[14] Madle PJ, Robinson WA. In situ method for measuring the permeability and resistivity of metal sheets IEEE Trans Instrum Meas 1975;24:300–5.
[15] Moosbrugger C, Cverna F. ASM ready reference: electrical and magnetic properties of metals. Materials Park: ASM International; 2000; 29.
[16] Thomas LC. Heat transfer. Tulsa: Capstone Publishing Corporation; 1999; 19.
[17] Lide DR. Handbook of chemistry and physics. Florida: CRC press; 1991; 1233–1235.